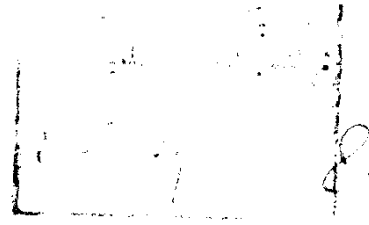
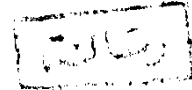


Ain Shams University  
Faculty of Sciences  
Geology Department



**GEOLOGIC AND RADIOMETRIC  
STUDIES OF GABAL NAAG AREA,  
SOUTHEAST ASWAN, EGYPT**

By



**ADEL AHMED FOUAD ABD EL-WAHED**

**Geologist in Nuclear Materials Authority**

**Cairo, Egypt**

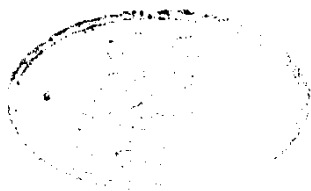
**B. Sc.-Very Good with Honors Degree,  
1985**

557.701  
A. A

8113

**A Thesis  
Submitted in Partial Fulfillment of  
the Degree of Master of Science in  
Geology**

**1994**



عبد الوهيد  
1994/6/21

## NOTE

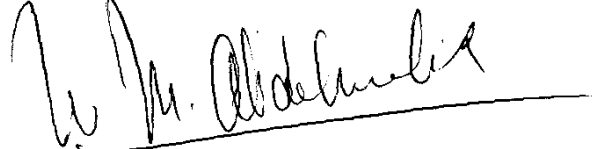
The present thesis is submitted to Geology Department, Faculty of Science, Ain Shams University in partial fulfillment for the requirements for the degree of Master of Science in Geology.

Beside the research work materialized in this thesis, the candidate: **Adel Ahmed Fouad Abd El-Wahed** has attended ten post - graduate courses for one year in the following topics:

- 1 - Mineralogy.
- 2 - Geochemistry.
- 3 - Igneous petrology.
- 4 - Metamorphic petrology.
- 5 - Sedimentary petrology.
- 6 - Sedimentation.
- 7 - Field geology and mapping.
- 8 - Geostatistics and introduction to Basic programming.
- 9 - Laboratory techniques.
- 10 - Ore petrology.

He has successfully passed the Final exam in the above mentioned courses, besides an English language course.

**Prof. Dr. W. Morcos**



Head of Geology Department

Faculty of Science

Ain Shams University



## **ACKNOWLEDGMENTS**

**Praise be to ALLAH, the Lord of the Worlds, by whose grace this work has been completed .**

**My deepest appreciations and gratitudes are due to Prof. Dr. A. I. Ragab, Geology Department, Faculty of Science, Ain Shams University, for supervision, valuable advice and critical comments while preparing the thesis .**

**I would like to express my gratitudes to Prof. Dr. A. F. Kamel, Head of Photogeology Department, NMA, for suggesting the point, supervising the work and kind encouragement .**

**I wish to express my deep thanks to Dr. H. A. Hussein, Head of Radiometry Lab., NMA, for supervision and valuable discussions .**

**The author would like to thank Prof. Dr. A. A. Abdel Moneim, Head of Research Sector, NMA, Prof. Dr. M. M. Aly, Prof. Dr. M. Y. Attawia, Dr. S.I. Mansour, Mr.H.K.Fouad, Mr. T. F. Mohammadien, Mr.S. Z. Tawfik and Mr.M.H.Attiea for the facilities they offered during the progress of this work .**

**Thanks are also extended to all members of the geologic group of Aswan camp for their cooperation during the field work .**

## CONTENTS

	<b>Page</b>
<b>LIST OF FIGURES</b>	<b>IV</b>
<b>LIST OF TABLES</b>	<b>XI</b>
<b>ABSTRACT</b>	<b>XII</b>
 <b>Chapter I</b>	
<b>INTRODUCTION</b>	<b>1</b>
 A - Location	1
B - Topography	1
C - Climate and water supplies	3
D - Previous work	3
E - Objective and scope of the present study	4
 <b>Chapter II</b>	
<b>GEOLOGICAL SETTING</b>	<b>7</b>
 1 - Ophiolitic mélange assemblage	9
1.1 Serpentinites	9
1.2 Ortho-amphibolites	9
1.3 Schists	9
1.4 Marbles	13
1.5 migmatitic gneisses	13
2 - Arc-metavolcanics	17
3 - Syn-collision granites	17
4 - Post granite dykes	20
a - Felsites	20
b - Quartz andesites	20
c - pegmatites	20
5 - Nubia sandstones	22
6 - Post Pan-African magmatism	22
7 - Wadi deposits	22

<b>Chapter III</b>		<b>Page</b>
	<b>PETROGRAPHY</b>	<b>26</b>
1 - Ophiolitic mélange assemblage		26
1.1 Serpentinites		26
1.2 Ortho-amphibolites		28
1.3 Schists		28
1.4 Marbles		28
1.5 Migmatitic gneisses		32
1.5.1 Biotite-quartz-oligoclase gneisses		32
1.5.2 Biotite-hornblende gneisses		32
1.5.3 Muscovite-quartz plagioclase gneisses		35
1.5.4 Garnet gneisses		35
1.5.5 Stromatic migmatites		38
2 - Arc-metavolcanics		38
3 - Syn-collision granites		38
4 - Post Pan-African magmatism		42
4.1 Basalts		42
4.2 Dolerites		42
<b>Chapter IV</b>		
	<b>GEOCHEMISTRY</b>	<b>47</b>
1 - Syn-collision granites		47
1.1 Petrochemical characters		47
1.2 Geotectonic environment		54
2 - Gneisses and migmatites		57
3 - Ortho-amphibolites		59
4 - Post Pan-African basalt		59
<b>Chapter V</b>		
	<b>RADIOMETRIC INVESTIGATIONS</b>	<b>63</b>
1 - Field radiometric measurements		63
2 - Radioactive anomalies		65
3 - Laboratory analysis		69

	<b>Page</b>
i - $\gamma$ ray spectrometric	69
ii - X ray diffraction	77
3 - Factors governing the distribution of radioactivity	77
a - Lithological control	77
b - Structural control	79
4 - Origin of radioactivity	79
5 - Uranium and thorium mineralization in the Southeastern Desert	80
 Chapter VI	
<b>DISCUSSION AND CONCLUSIONS</b>	<b>82</b>
 <b>REFERENCES</b>	<b>94</b>
<b>ARABIC SUMMARY</b>	<b>104</b>

## LIST OF FIGURES

Figure No.		Page
1	Location map of Gabal Naag area in a sketch map showing the distribution of ultramafic rocks and gneisses in the Eastern Desert of Egypt (after Ragab and El-Gharabawi, 1989) .	2
2	Geological map of Gabal Nasyia area (after Armanious et. al., 1977) .	5
3	Simplified geologic map from the geologic map of Egypt (After Geological Survey with Egyptian General Petroleum Corporation, 1987) .	5
4	Geological map of Gabal Naag area, Southeastern Desert, Egypt .	8
5	View showing ortho-amphibolites within migmatitic gneisses at the northern part of Gabal Naag area .	10
6	View showing Nubia sandstones overlying ortho-amphibolites at the southern part of Gabal Naag area .	10
7	View showing the parallel foliation of the migmatitic gneisses and ortho-amphibolites at Gabal Naag area .	11
8	View showing Nubia sandstones overlying the schists and the arc metavolcanics at the southeastern part of the Gabal Naag area .	11
9	View showing the foliation of the schists and the arc metavolcanics at the southeastern part of Gabal Naag area .	12
10	View showing marble band within the migmatitic gneisses at the eastern part of Gabal Naag area .	12

<b>Figure No.</b>		<b>Page</b>
11 (a)	Rose diagram showing the relative strike frequencies of foliation in the schists .	14
(b)	Stereogram for 106 foliation planes in schists, Gabal Naag area.	
12 (a)	Rose diagram showing the relative strike frequencies of foliation in the migmatitic gneisses .	14
(b)	Stereogram for poles of 295 foliations in the migmatitic gneisses, Gabal Naag area .	
13 (a)	Rose diagram showing the relative strike frequencies of joints in syn-collision granites .	14
(b)	Stereogram for poles of 186 joints in syn-collision granites .	
14	View showing marble band within the migmatitic gneisses at the eastern part of Gabal Naag area .	15
15	View showing stromatic migmatite at the northern part of Gabal Naag area .	15
16	View showing stromatic migmatite at the eastern part of Gabal Naag area .	16
17	View showing microfold in the migmatitic gneisses at the northern part of Gabal Naag area .	16
18	View showing well developed foliated migmatitic gneisses at Gabal Naag area .	18
19	View showing Nubia sandstones overlying arc-metavolcanics of Gabal Musrar at the southeastern part of Gabal Naag area .	18
20	View showing syn - collision granites covered by Nubia sandstones .	19
21	View showing syn - collision granites capped by Nubia sand-	19

Figure No.		Page
	stones at the southwestern part of Gabal Naag area .	
22	View showing pegmatite vein in the syn-collision granites at Gabal Naag area .	21
23	View showing quartz vein in the syn-collision granites at Gabal Naag area .	21
24	View showing post Pan-African basalt flow at Wadi El-Quffa .	23
25	View showing post Pan-African basalt flows at Wadi El-Quffa.	24
26	Photomicrograph of serpentinites showing opaques and antigorite fibers .	27
27	Photomicrograph of serpentinites showing cross fibers antigorite vein .	27
28	Photomicrograph of ortho - amphibolite showing zircon crystals, hornblende and plagioclase .	29
29	Photomicrograph of ortho - amphibolite showing enclosed plagioclase and quartz crystals within psimatic crystal of hornblende forming poikilitic texture .	29
30	Photomicrograph of foliated ortho - amphibolite showing parallel orientation of hornblende crystals .	30
31	Photomicrograph of ortho - amphibolite showing hornblende, epidote and plagioclase .	31
32	Photomicrograph of a schist showing quartz, muscovite and magnetite .	31
33	Photomicrograph of forsterite marble showing calcite and	33

Figure No.		Page
	euhedral crystal of olivine .	
34	Photomicrograph of brucite marble showing clearly the rhombohedral cleavage in anhedral calcite and brucite .	33
35	Photomicrograph of biotite gneiss showing scattered biotite flakes .	35
36	Photomicrograph of biotite gneiss showing rounded quartz grain and biotite flakes within oligoclase forming a poikilitic texture .	36
37	Photomicrograph of biotite-hornblende gneiss showing biotite, hornblende, quartz and subhedral crystals of oligoclase .	36
38	Photomicrograph of muscovite gneiss showing porphyroblasts of oligoclase with well developed lamellar twinning .	37
39	Photomicrograph of garnet gneiss showing crystal of garnet .	37
40	Photomicrograph of stromatic migmatite showing biotite flakes, altered oligoclase and microcline .	39
41	Photomicrograph of arc - metavolcanics showing euhedral phenocrysts of oligoclase, altered flakes of biotite, quartz in microcrystalline matrix .	39
42	Photomicrograph of syn - collision granites showing graphic intergrowth textures .	40
43	Photomicrograph of syn - collision granites showing euhedral rhombic sphene crystal .	40
44	Photomicrograph of syn - collision granites showing euhedral allanite crystal .	41

<b>Figure No.</b>		<b>Page</b>
45	Photomicrograph of syn - collision granites showing fine squeezed aggregates of quartz between microcline and plagioclase .	41
46	Photomicrograph of syn-collision granites showing cross hatching twinning in microcline, quartz and altered oligoclase .	43
47	Photomicrograph of syn-collision granites showing epidote, quartz, biotite and saussuritized plagioclase .	43
48	Photomicrograph of syn-collision granites showing crystals of biotite, quartz and altered oligoclase .	44
49	Photomicrograph of post Pan - African basalt showing partly altered olivine phenocrysts and lath-shaped plagioclase .	44
50	Photomicrograph of post Pan-African basalt showing phenocrysts of augite and olivine in a matrix of andesine to labradorite laths, augite, biotite, hornblende and magnetite .	45
51	Photomicrograph of post Pan-African dolerite showing plagioclase laths (labradorite), pyroxene (augite), hornblende and magnetite .	45
52	(Na <sub>2</sub> O+K <sub>2</sub> O) versus SiO <sub>2</sub> diagram for syn-collision granites .	49
53	AFM for the examined syn-collision granites .	49
54	Variation diagram of the different oxides percentages against the differentiation index .	51
55	Variation diagram for ( Na <sub>2</sub> O + K <sub>2</sub> O ) and for (CaO) versus (SiO <sub>2</sub> ) of the examined syn-collision granites .	52
56	Variation in alkalis of syn-collision granites .	52

<b>Figure No.</b>		<b>Page</b>
57	Rittmann suite index for the syn-collision granites .	53
58	Normative Q-Ab-Or diagram for syn-collision granites .	53
59	Normative An-Ab-Or diagram for the syn-collision granites .	55
60	Nb-SiO <sub>2</sub> plots of the syn-collision granites .	55
61	Ta versus Yb for discrimination between syn-collision, volcanic arc, within plate and oceanic ridge granites .	56
62	ACF diagram for the examined gneisses, migmatites and ortho-amphibolites .	61
63	( Na <sub>2</sub> O + K <sub>2</sub> O ) - SiO <sub>2</sub> plots of Gabal Naag Post Pan-African basalts .	62
64	Radiometric contour map of Gabal Naag area , southeast Aswan, Egypt .	64
65	Histogram showing the distribution of gamma radioactivity in (c.p.s.) for the different rock units in Gabal Naag area .	67
66	Geologic section and radiation intensity profile across rocks of Gabal Naag area .	68
67	U distribution in anomalous granite determined by gamma ray spectrometry .	74
68	Th distribution in anomalous granite determined by gamma ray spectrometry .	74
69	K distribution in anomalous granite determined by gamma ray spectrometry .	75

<b>Figure No.</b>		<b>Page</b>
70	Th / U ratio distribution in anomalous granite determined by gamma ray spectrometry .	75
71	The U - Th relationship in syn-collision granites of Gabal Naag area .	76
72 (a)	Th / U - U relationship in syn-collision granites of Gabal Naag area .	76
(b)	Th / U - Th relationship in syn-collision granites of Gabal Naag area .	
73	Frequency histogram of U-K in syn-collision granites of Gabal Naag area .	78
74	Frequency histogram of U-Th in syn-collision granites of Gabal Naag area .	78
75	Generalized cross-section of intra-oceanic island arc, forearc-trench system and backarc marginal ocean basin .	91
76	Classification of forearc basins .	91
77	Plate tectonic model for the crustal growth and orogenic migration of Gabal Naag area .	93

## LIST OF TABLES

Table No.		Page
1	Data of complete chemical analyses and CIPW of syn-collision granites .	48
2	Chemical analyses of gneisses and migmatites from Gabal Naag area and average analyses for comparison .	58
3	Chemical analyses of ortho - amphibolites and post Pan-African basalt from Gabal Naag area .	60
4	Radioactivity at the different types of rocks at Gabal Naag area .	66
5	Radioelements concentrations of the syn-collision granites in Gabal Naag area .	70
6	Radioelements concentrations in crustal rocks ( After IAEA, 1979 and Boyle, 1982) .	72
7	Comparison between some favourable host mineralization, Southeastern Desert, Egypt .	81
8	Tectonostratigraphy of Gabal Naag area .	89